

Vibration Analysis of Carbon Nanotubes Based on Cylindrical Shell by Inducting Winkler and Pasternak Foundations



By

Shahid Mubbashir

(226-FBAS/MSMA/F14)

**Department of Mathematics and Statistics
Faculty of Basic and Applied Sciences
International Islamic University Islamabad
Pakistan**

2017

ii





Accession No

TH:18716 ^{1/2/21}

MS

620.5

SHY

Nanotechnology

Nanotubes.

Nanostructured materials.

Vibration Analysis of Carbon Nanotubes Based on Cylindrical Shell by Inducting Winkler and Pasternak Foundations



Submitted by

Shahid Mubbashir

(226-FBAS/MSMA/F14)

Supervised by

Dr. Ahmed Zeeshan

**Department of Mathematics and Statistics
Faculty of Basic and Applied Sciences
International Islamic University Islamabad
Pakistan
2017**

Vibration Analysis of Carbon Nanotubes Based on Cylindrical Shell by Inducting Winkler and Pasternak Foundations

Author

Shahid Mubbashir

A dissertation

Submitted in partial fulfillment of the

Requirements for the degree of

MASTER OF SCIENCE

IN

MATHEMATICS

Supervised by

Dr. Ahmed Zeeshan

**Department of Mathematics and Statistics
Faculty of Basic and Applied Sciences
International Islamic University Islamabad
Pakistan
2017**

Certificate


Vibration Analysis of Carbon Nanotubes Based on Cylindrical Shell by Inducting Winkler and Pasternak Foundations

By


Shahid Mubbashir

A DISSERTATION SUBMITTED IN THE PARTIAL FULFILLMENT OF THE REQUIREMENTS
FOR THE DEGREE OF THE MASTER OF SCIENCE IN STATISTICS


We accept this dissertation as conforming to the required standard.

1. 

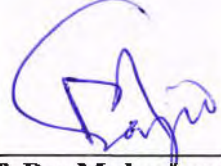
Dr. Hafiz Obaid Ullah Mehmood
External Examiner

2. 

Dr. Nasir Ali
Internal Examiner

3. 

Dr. Ahmed Zeeshan
Supervisor

4. 

Prof. Dr. Muhammad Sajid, T.I
Chairman

**Department of Mathematics & Statistics
Faculty of Basic and Applied Sciences
International Islamic University, Islamabad
Pakistan
2017**

Dedicated To
My Sweet Mother and Loving Father

Declaration

I certify that this research work is my own work and it has not been presented elsewhere for assessment. The material that has been used from other sources is properly acknowledged / referred.

Signature of Student

Shahid Mubbashir

Acknowledgements

I humbly prostrate to **Allah the Almighty** who created me, brought me up, taught me and enabled me to compile this thesis.

I offer sincere gratitude to my cherished parents and siblings with whom love my childhood became finest, with whom pains my all wishes came to true, with whom prays the exams of my life converted into ease. I proudly signify the support and cherish from my brothers Abid Farooq and Rashid Umer.

I am very grateful to my supervisor **Dr. Ahmed Zeeshan** whose encouragement, valuable ideas, and words of advice both morally and mathematically proved for me a great assistance to nourish my abilities and made me capable to face the challenges with firm determination. I also take the opportunity to thank and prays for my all teachers who taught me.

I am very thankful to **Dr. Aaqib Majeed** who helped me well and where ever I faced dilemma in research work he guided me on the right way. Moreover, his continuous support and valuable ideas enabled me to write a research article, as well. I am also grateful to my research fellows and friends (Muhammad Muddassar Maskeen, Farooq Hussain, Nouman Ejaz, Nasir shehzad, Bilal Arain, Shahid Nadeem, Zeeshan Pervaiz, Kashif Choudhary, M.Luqman, Arif Hussain, Fehad, Amad Ur Rehman, Aftab Ahmed, Usman Ali, Muddasir Rehman, Sajad Ahmed, Iqrar Raza and Muhammad Awais etc) for providing me a kind companionship in bundle of meetings and parties.

Shahid Mubbasher

Preface

Understanding of the vibrational properties of the carbon nanotubes (CNTs) and their uses have been involved in various areas such as electronics, optics, medicine, charge detectors, sensors, field emission devices, aerospace, defence, construction and even fashion. Iijima [1] Investigated CNTs remarkable properties, a bulk of research work was performed for their high springiness and characteristic ratio. Falvo et al. [2] found a very effective Young modulus and tensile potency. Li and Chou [3] analysed well-bonding strength and superconductivity between carbon atoms. Sakhaee et al. [4] discussed vibrations of CNTs. Vibration of CNTs have been studied extensively in the last fifteen years and various cost effective continuum models such as thin shell, [5] beam and [6] ring, [7] as well as other continuum models. Li and Chou [3] and Cao et al. [8] have been proposed to capture the new physical phenomena and quantified the mechanical properties and identified the major factors that effect the mechanical behaviour of CNTs. Chapter 2 comprises on vibration analysis of a cylindrical shell i.e. natural frequency of the cylindrical based shell is investigated for simply supported-simply supported (S-S) boundary condition. The equations of motion of cylindrical shell are taken by employing Love's first approximation shell theory which are then solved numerically by using wave propagation approach. The obtained results of the natural frequencies are confirmed with those in previously published literature. Chapter 3 comprises on the vibrational analysis of CNTs of different shapes by using different boundary conditions.

Contents

Chapter 1: Introduction	03
1.1 Vibration	03
1.1.1 Frequency and Time Period	03
1.1.2. Wave Number	04
1.2 Boundary Conditions	04
1.3 Elastic Foundation.....	06
1.3.1 Winkler Foundation	06
1.3.2 Pasternak Foundation.....	06
1.4 Carbon Nanotube.....	07
1.4.1 Introduction.....	07
1.4.2 Structure of CNTs	07
1.4.3. Types of CNTs.....	08
1.4.4 Applications of CNTs.....	11
1.5 Wave Propagation Approach.....	12
1.6 Literature Review.....	13
Chapter 2: Vibrational Analysis of Cylindrical Shell.....	16
2.1 Introduction	16
2.2 Mathematical Formulation of Equations of Motion.....	16
2.3 Solution Methodology	19
2.4 Results and Discussions	21
2.5 Conclusion.....	25

Chapter 3: Vibrational Analysis of Carbon Nanotubes Based on Cylindrical Shell By Inducting Winkler and Pasternak Foundations	26
3.1 Introduction	26
3.2 Mathematical Formulation of Equations of Motion	26
3.3 Solution Methodology	27
3.4 Results and Discussions.....	30
3.5 Conclusion	38
References:	39

Chapter 1

Introduction

1.1 Vibration

Vibration is a mechanical phenomenon whereby oscillations occur about an equilibrium point. The word comes from Latin *vibrationem* (shaking, brandishing). The oscillations may be periodic, such as the motion of a pendulum or random, such as the movement of a tire on a gravel road. Some important notations and nomenclature are defined in the subsequent sections.

1.1.1 Frequency and Time Period

Frequency is the number of occurrences of a repeating event per unit time. Whereas the period is the duration of time of one cycle in a repeating event, so the period is the reciprocal of the frequency. For example, if a new born baby's heart beats at a frequency of 120 times a minute, its period is half a second, i.e. 60 seconds divided by 120 beats. Frequency is an important parameter used in science and engineering to specify the rate of oscillatory and vibratory phenomena, such as mechanical vibrations, audio (sound) signals, radio waves and light. The frequency at which a system tends to oscillate in the absence of any driving or damping force or one can say the frequency at which a system oscillates subjected to no external force is named as natural frequency.

1.1.2 Wave Number

The wave number is the spatial frequency of a wave, either in cycles per unit distance or radians per unit distance. It can be imagined as the number of waves that exist over a specified distance. In multidimensional systems, the wavenumber is the magnitude of the wave vector. The space of wave vectors is called reciprocal space. Wave numbers and wave vectors play an essential role in optics and the physics of wave scattering. The specified distance of waves in the circumferential direction is specified as a circumferential wave number.

1.2 Boundary Conditions

1.2.1 Free-Free Boundary Condition (F-F)

Free-free boundary conditions are one where the rotation and shear is zero in the mid of the beam, rod or cylinder. At the edges the moments are equal to zero and edge deflection and edge slopes are both equal to zero.



Fig. (1.1)

1.2.2 Clamped-Clamped Boundary Condition (C-C)

The boundary condition for a clamped-clamped cylinder generally indicate that the edge deflection and edge slopes are both equal to zero.

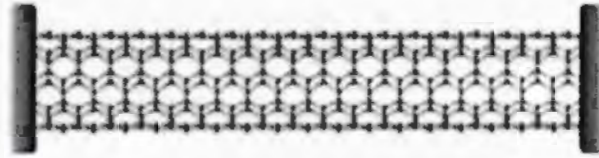


Fig. (1.2)

1.2.3 Clamped-Free Boundary Condition (C-F)

The boundary condition for a clamped-Free cylinder generally indicate that the edge deflection and edge slopes are both equal to zero at one end of the cylinder but not zero on the other end.

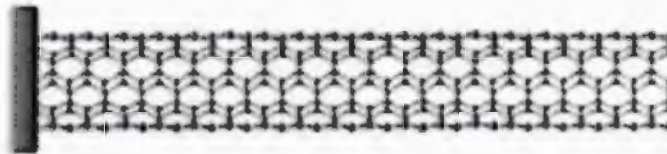


Fig. (1.3)

1.2.4 Clamped-Sliding Boundary Condition (C-Sl)

The boundary condition for a clamped-sliding cylinder generally indicate that the edge deflection and edge slopes are both equal to zero at one end of the cylinder and edge slopes is not zero on the other end.

1.2.5 Simply Support-Simply Support Boundary Condition (S-S)

The boundary condition for a Simply Support-Simply Support cylinder generally indicate that the edge deflection is equal to zero but edge slopes can vary depending upon the load at both ends.

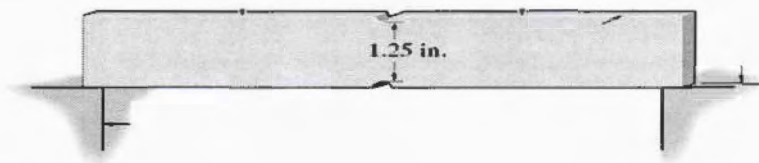


Fig. (1.4)

1.3 Elastic Foundations

1.3.1 Winkler Foundation

One very popular method for modelling the soil structure interaction has its origins in the work done by Winkler in 1867 where the vertical translation of the soil W at a point is assumed to depend only upon the contact pressure P acting at that point in the idealized elastic foundation and a proportionality constant K .

$$KW = P. \quad (1.1)$$

The proportionality constant K is commonly called the modulus of subgrade reaction or the coefficient of subgrade reaction. This model was first used to analyse the deflections of resultant stresses in railroad tracks. In the intervening years, it has been applied to many different soil-structure and interaction problems, and it is known as the Winkler model.

1.3.2 Pasternak Foundation

In Pasternak foundation model the springs are coupled with one another. This model is also known as a two parameter model because it takes another term into account. This term is the G parameter. Physically, this parameter represents the interaction due to shear action among the spring elements. With this extra parameter the displacement of

the model can be more realistic as compared to the one parameter model i.e. Winkler model.

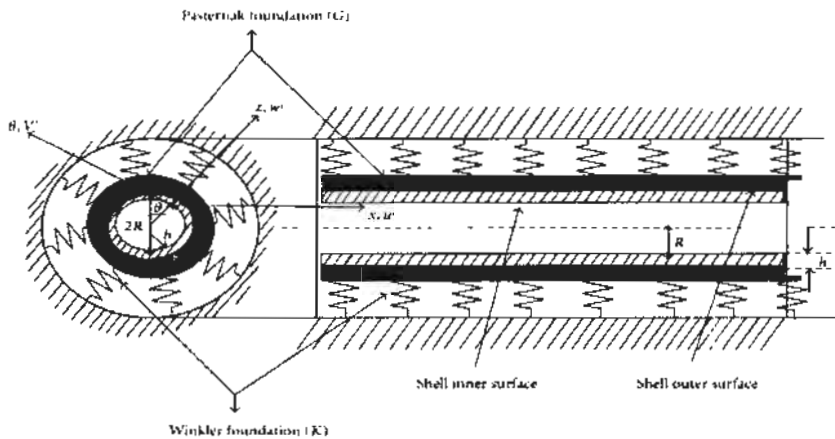


Fig. (1.5)

1.4 Carbon Nanotubes

1.4.1 Introduction

Coal and diamonds, sand and computer chips, cancer and healthy tissues: variations in the arrangement of atoms have distinguished the cheap from the cherished, the diseased from the healthy. Arranged one way the atoms make up soil, air and water. Arranged in the other way they make ripe strawberries. Arranged one way they make up homes and fresh air, arranged another they make up ash and smoke. Our ability to arrange atoms lies at the foundation of nanotechnology Iijima discovered CNTs in 1991. The prefix “nano” corresponds to a basic unit on a length scale, meaning 10^{-9} meters, which is a hundred to a thousand times smaller than a typical biological cell or bacterium. CNTs have a variety of applications because of their distinctive molecular structure and their fascinating mechanical and electrical properties.

1.4.2 Structure of CNTs

The structure of CNTs can be considered as arising from the folding of one or more layers of graphite to form a cylinder composed of carbon hexagons. These nanotubes have a hemispherical "cap" at each end of the cylinder as shown in the Fig. 1.6. They are light, flexible and thermally stable and are chemically inert.

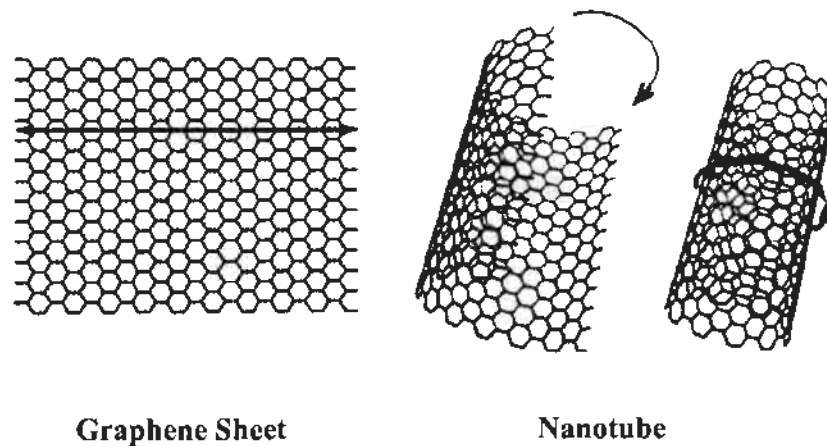


Fig. 1.6. Formation of CNT from graphene sheet

Nanotubes are composed entirely of sp^2 bonds which are stronger than the sp^3 bonds found in diamond. This bonding structure provides them with their unique strength. Nanotubes align themselves into ropes held together by van der Waals force. Under high pressure, nanotubes can merge together, trading some sp^2 bonds for sp^3 bonds, giving great possibility for producing strong, unlimited-length wires through high-pressure nanotubes linking.

1.4.3 Types of CNTs

Basically nanotubes are two types depending upon the layers as shown in Fig. 1.7.

They are

1. Single walled nanotube (SWNT)
2. Multi walled nanotube (MWNT)

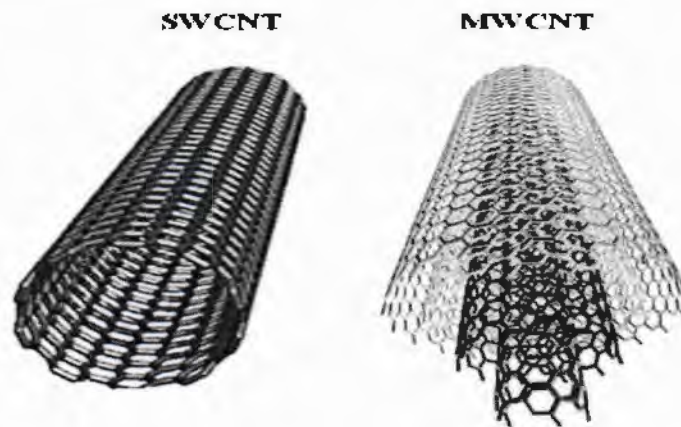


Fig. 1.7. Single and multi-walled nanotubes

Nanotubes can be categorized into three types according to their structure. They are

- i. Arm-Chair
- ii. Chiral
- iii. Zigzag

Nanotubes form different types, which can be described by the chiral vector (n, m) , where n and m are integers of the vector equation $C_h = na_1 + ma_2$. The chiral vector is determined as shown by the Fig. 1.8. Imagine that the nanotube is unravelled into a planar sheet. Draw two continuous lines along the tube axis where the separation takes place. In other words, if we cut along the two continuous solid lines and then match their ends together in a cylinder, you get the nanotube that you started with. Now, find any point on one of the thick black lines that intersects one of the carbon atoms (point A). Next, draw the Armchair line (n, n) which travels across each hexagon, separating them into two equal halves. Now that you have the armchair line drawn, find a point

along the other tube axis that intersects a carbon atom nearest to the Armchair line (point B).

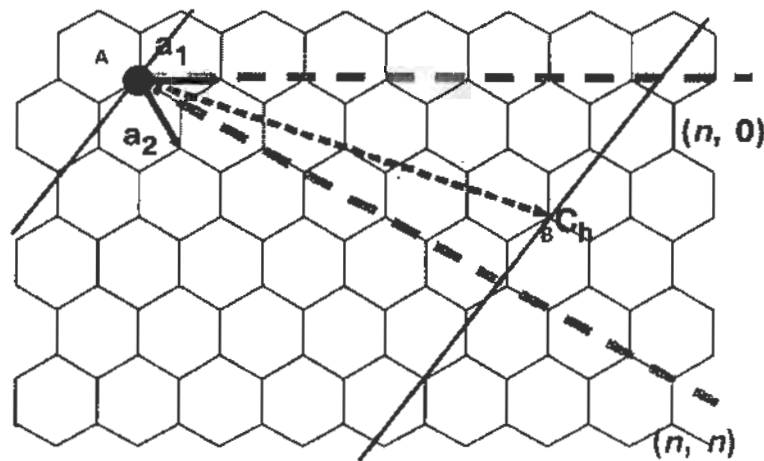


Fig. 1.8. Chiral vector of a nanotube

Now connect A and B with our chiral vector C_h . The wrapping angle α (not shown) is formed between C_h and the Armchair line. If C_h lies along the Armchair line ($\alpha=0^\circ$), then it is called an "Armchair" nanotube. If $\alpha=30^\circ$, then the tube is of the "zigzag" type. Otherwise, if $\alpha \ll 30^\circ$ then it is a "chiral" tube. The values of n and m determine the chirality, or "twist" of the nanotube. The chirality in turn affects the conductance of the nanotube, its density, its lattice structure, and other properties. Fig. 1.9 shows the different types of carbon nanotubes according to their structure.

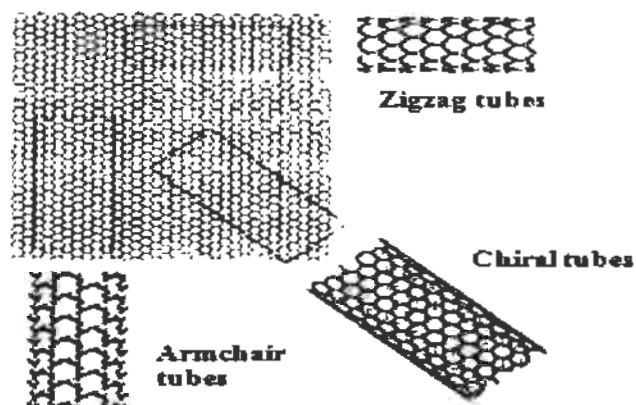


Fig. 1.9. Different wrapping to form nanotube.

1.4.4 Applications of CNTs

CNTs exhibit unique electronic and mechanical properties because of their curvature. Because of their inimitable properties, CNTs find a number of interesting applications in different fields of engineering. Some of the applications discussed by Ajayan and Zhou [9] are as follows:

- a. Carbon nanotubes have the right combination of properties i.e. nanometer size diameter, structural integrity, high electrical conductivity, and chemical stability that makes good electron emitters.
- b. Prototype matrix-addressable diode flat panel displays can be fabricated using CNTs as the electron emission source.
- c. Nanotubes can be used as reinforcements in composite materials. Nanotube reinforcements will increase the toughness of the composites by absorbing energy during their highly flexible elastic behaviour.
- d. Nanotube filled polymers can be used in electromagnetic induction (EMI) shielding applications.
- e. Because of its hollow geometry and nano scale diameter, it has been predicted that the carbon nanotubes can store liquid and gas in the inner cores through a capillary effect.
- f. CNT's because of their extremely small sizes, high conductivity, high mechanical strength and flexibility, they are used in electrical instruments as well as other scanning probe instruments, such as an electrostatic force microscope.
- g. MWCNT and SWCNT tips were used in a tapping mode to image biological molecules such as amyloid-b-protofibrils with resolution never achieved before.

- h. Nanotubes with controlled helicities could be used as unique probes for molecular recognition, based on the helicity and dimensions, which are recognized by organic molecules of comparable length scales.
- i. CNTs have relatively straight and narrow channels in their cores which can be filled with foreign materials to fabricate one-dimensional nanowires.
- j. Since the electrical resistivity of SNWTs were found to change sensitively on exposure to gaseous ambient, hence CNTs can be used as chemical sensors.

They can be used to dissipate heat from tiny computer chips. Nanotube composite motor brushes are better lubricated, stronger and more accurately mouldable. CNTs have already been used as composite fibres in polymers and concrete to improve their mechanical, thermal and electrical properties of the bulk product. Nanotubes are critical material that enables construction of space elevators from earth to geosynchronous orbit. Gao [10] found that CNTs have the highest reversible capacity of any carbon material for use in lithium-ion batteries. Because of their negligible weight, they find application in space applications. Since nanotubes are similar scale size of DNA, promising possibilities can be expected by introducing them to reinforce tissue scaffolds. CNTs have a high surface area and their ability to attach to any chemical species to their sidewalls provides an opportunity for unique catalyst supports.

1.5 Wave Propagation Approach

For the present study, the wave propagation approach is employed to analyse the vibration characteristics of cylindrical shells. This approach is very simple and easily applicable to determine the shell frequencies and has been successfully applied by a

number of researchers. For separating the spatial and temporal variables, the following shapes of modal displacement functions are assumed:

$$u(x, \theta, t) = A \cos(n\theta)e^{i(\omega t - k_m x)},$$

$$v(x, \theta, t) = B \sin(n\theta)e^{i(\omega t - k_m x)},$$

$$w(x, \theta, t) = C \cos(n\theta)e^{i(\omega t - k_m x)},$$

in the axial, circumferential and radial directions, respectively. The coefficients A, B and C denote the wave amplitudes respectively in the x, θ and z directions, respectively. n is the number of circumferential waves and K_m is the axial wave number that has been specified for a number of boundary condition. These axial wave numbers K_m are chosen to satisfy the required boundary conditions at the two ends of the vibrational characteristics of cylindrical shells. ω is the natural circular frequency of the cylindrical shell. On substituting these expressions u, v and w in the governing equations and simplifying those algebraic expressions and rearranging the terms, the frequency equation is written in the form of eigenvalue problem. On solving this Eigen value problem by using some computer software the three frequencies are obtained corresponding to the axial, circumferential and radial displacements.

1.6 Literature Review

Investigations of free vibration of CNTs have been examined with regard to their properties and material behaviour. For practical applications, it needs more exploration to examine vibration characteristics of single-walled carbon nanotubes (SWCNTs). Moreover, vibration properties of CNTs have significant role in material strength analysis and have practical importance. A reliable knowledge of vibrational data is also important for an optimized design of processes and apparatus in various engineering

and science fields (for instance electrical, biological sciences and chemical engineering). New innovative improvement and technologies such as nano-probes, emanation panel spectacle, nano-electronics, and chemical sensing and drug deliverance have been proposed. Vibration problems of SWCNTs can be investigated experimentally, theoretically and by simulation techniques. Poncharal et al. [11] and Treacy et al. [12] performed experiment to calculate the resonance frequency of multi-walled CNTs (MWCNTs) for clamped-free excited by electrical loads or thermal process. Zhao et al. [13] applied molecular dynamics (MD) simulations for the investigations of natural frequencies and to predict the Young's modulus. Moreover, Hsu et al. [6] reported the resonant frequency for CNTs model of chiral SWCNTs and these tubes are observed under a thermal vibration. The Timoshenko beam model (TBM) has been used for implicating the shear deformation and rotatory inertia of CNTs and nonlocal theory (NLT) of elasticity is employed for the vibration analysis of SWCNTs. Molecular structural mechanics (MSM) method of Li and Chou [14] has been employed in order to understand the feasibility of SWCNTs as a Nano resonator. The measured fundamental frequencies were perceptive to dimensions such as diameter and length along with boundary conditions (clamped-free or clamped) of SWCNTs. The static and dynamics properties of CNTs are computed by using MSM method successfully Li Chunyu et al. [15] and the natural frequencies of SWCNTs are investigated in Refs. C. Y. Li et al. [16] and Li Chunyu [15]. Gibson et al. [17] investigated high fundamental frequencies of 10~300GHz (and 100~1500 GHz) at length-to-diameter of 6~20 nm (0.4~0.8 nm), respectively, for CNTs. Chirality of nanotubes does not have a momentous effect on the fundamental frequency, however, CNTs have higher values of fundamental frequency at the lower values of diameter. Another research group with armchair and zigzag CNTs investigated the fundamental

frequency with different values of length-to-diameter ratio. Swain et al [18] concluded that zigzag CNTs have higher frequencies than armchair CNTs. Moreover, continuum mechanics models depicted that thickness and Young's modulus of CNTs plays a significant role for vibrational analysis of nanotubes. In addition, Fereidoon et al. [19] performed the analysis of a (CNT) reinforced polymer using a 3D finite-element model and constructed a non-bonded interphase region and the surrounding polymer with multi scale finite-element model.

Chapter 2

Vibrational Analysis of Cylindrical Shell

2.1 Introduction

This chapter comprises on the natural frequency of the cylindrical shell investigated for simply supported (S-S) boundary condition by using wave propagation approach. The equations of motion for cylindrical shell are taken from Love's thin shell theory.

2.2 Mathematical Formulation of Equations of Motion

Consider a cylindrical shell having geometrical parameter length, radius, and thickness denoted by L, R, h respectively. The cylindrical shell has material properties Young's modulus, poisson ratio and mass density represented by E, ν, ρ respectively. An orthogonal coordinate system is established in the middle of the cylindrical shell for representation of axial, circumferential and radial displacements denoted by x, θ and z . While u', v' and w' are the displacements in the axial, circumferential and radial directions respectively.

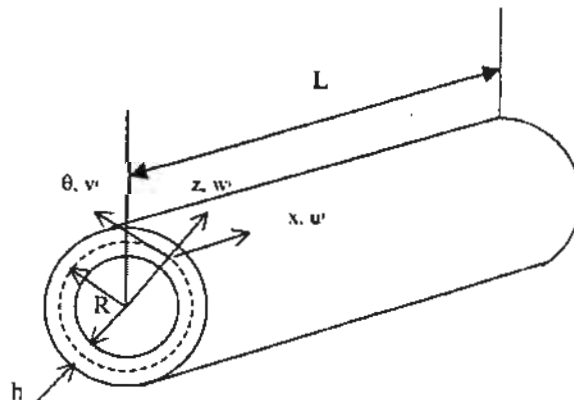


Fig. 2.1. Cylindrical shell furnished with geometrical parameters.

The equations of motion (2.1)-(2.3) are obtained by using Love's theory of the shell.

$$\frac{\partial N_x}{\partial x} + \frac{1}{R} \frac{\partial N_{x\theta}}{\partial \theta} = \rho h \frac{\partial^2 u'}{\partial t^2}, \quad (2.1)$$

$$\frac{\partial N_{x\theta}}{\partial x} + \frac{1}{R} \frac{\partial N_\theta}{\partial \theta} + \frac{2}{R} \frac{\partial M_{x\theta}}{\partial x} + \frac{1}{R^2} \frac{\partial M_\theta}{\partial \theta} = \rho h \frac{\partial^2 v'}{\partial t^2}, \quad (2.2)$$

$$\frac{\partial^2 M_x}{\partial x^2} + \frac{2}{R} \frac{\partial^2 M_{x\theta}}{\partial x \partial \theta} + \frac{1}{R^2} \frac{\partial^2 M_\theta}{\partial \theta^2} - \frac{N_\theta}{R} = \rho h \frac{\partial^2 w'}{\partial t^2}, \quad (2.3)$$

where $N_x, N_\theta, N_{x\theta}$ and $M_x, M_\theta, M_{x\theta}$ represent force resultant and moment resultant respectively. Which are defined in the literature as

$$\begin{Bmatrix} N_x \\ N_\theta \\ N_{x\theta} \\ M_x \\ M_\theta \\ M_{x\theta} \end{Bmatrix} = \begin{bmatrix} A'_{11} & A'_{12} & 0 & B'_{11} & B'_{12} & 0 \\ A'_{12} & A'_{22} & 0 & B'_{12} & B'_{22} & 0 \\ 0 & 0 & A'_{66} & 0 & 0 & B'_{66} \\ B'_{11} & B'_{12} & 0 & D'_{11} & D'_{12} & 0 \\ B'_{12} & B'_{22} & 0 & D'_{12} & D'_{22} & 0 \\ 0 & 0 & B'_{66} & 0 & 0 & D'_{66} \end{bmatrix} \begin{Bmatrix} e_1 \\ e_2 \\ \gamma \\ k_1 \\ k_2 \\ 2\tau \end{Bmatrix}, \quad (2.4)$$

where e_1, e_2, γ and k_1, k_2, τ represent the reference surface strains and the surface curvatures, respectively. Whereas A'_{ij}, B'_{ij} and D'_{ij} ($i, j = 1, 2$ and 6) are the membrane, coupling and flexural stiffness and given as

$$\{A'_{ij}, B'_{ij}, D'_{ij}\} = \int_{-h/2}^{h/2} Q_{ij} \{1, z, z^2\} dz. \quad (2.5)$$

To represent reduced stiffness which is due to an isotropic material, define

$$Q_{11} = Q_{22} = \frac{E}{1 - \nu^2}, \quad Q_{12} = \frac{\nu E}{1 - \nu^2}, \quad Q_{66} = \frac{E}{2(1 + \nu)}, \quad (2.6)$$

where Q_{ij} is reduced stiffness and $i, j = 1, 2$ and 6 . The ratio thickness to radius (h/R) of thin walled cylindrical based shell is less than 0.05. This ratio has an impact upon the natural frequency. There are number of theories to describe the motion of shell.

Only Love's theory is being discussed here to study vibrational behaviour of cylindrical shell. Love's theory define relationship between strain-displacement and curvature-displacement which are given as

$$\{e_1, e_2, \gamma\} = \left\{ \frac{\partial u'}{\partial x}, \frac{1}{R} \left(\frac{\partial v'}{\partial \theta} + w' \right), \left(\frac{\partial v'}{\partial x} + \frac{1}{R} \frac{\partial u'}{\partial \theta} \right) \right\}, \quad (2.7)$$

$$\{k_1, k_2, \tau\} = \left\{ -\frac{\partial^2 w'}{\partial x^2}, -\frac{1}{R^2} \left(\frac{\partial^2 w'}{\partial \theta^2} - \frac{\partial v'}{\partial \theta} \right), -\frac{1}{R} \left(\frac{\partial^2 w'}{\partial x \partial \theta} - \frac{\partial v'}{\partial x} \right) \right\}, \quad (2.8)$$

where e_1, e_2, γ and k_1, k_2, τ are strains and curvatures of the reference surface respectively. These parameters are then replaced into Eq. (2.4) and find the terms $N_x, N_\theta, N_{x\theta}, M_x, M_\theta, M_{x\theta}$ and put into the Eq. (2.1)-(2.3). The equation (2.9) represent motion for a cylindrical shell in the form,

$$\left. \begin{aligned} L_{11}u' + L_{12}v' + L_{13}w' &= \rho_t \frac{\partial^2 u'}{\partial t^2} \\ L_{21}u' + L_{22}v' + L_{23}w' &= \rho_t \frac{\partial^2 v'}{\partial t^2} \\ L_{31}u' + L_{32}v' + L_{33}w' &= \rho_t \frac{\partial^2 w'}{\partial t^2} \end{aligned} \right\}, \quad (2.9)$$

where $L_{ij} (i, j = 1, 2, 3)$ are differential operators and defined as:

$$L_{11} = A'_{11} \frac{\partial^2}{\partial x^2} + \frac{A'_{66}}{R^2} \frac{\partial^2}{\partial \theta^2},$$

$$L_{12} = \frac{(A'_{12} + A'_{66})}{R} \frac{\partial^2}{\partial x \partial \theta} + \frac{(B'_{12} + 2B'_{66})}{R^2} \frac{\partial^2}{\partial x \partial \theta},$$

$$L_{13} = \frac{A'_{12}}{R} \frac{\partial}{\partial x} - B'_{11} \frac{\partial^3}{\partial x^3} - \frac{(B'_{12} + 2B'_{66})}{R^2} \frac{\partial^3}{\partial x \partial \theta^2},$$

$$L_{21} = \frac{(A'_{12} + A'_{66})}{R} \frac{\partial^2}{\partial x \partial \theta} + \frac{(B'_{12} + 2B'_{66})}{R^2} \frac{\partial^2}{\partial x \partial \theta},$$

$$L_{22} = \left(A'_{66} + \frac{3B'_{66}}{R} + \frac{4D'_{66}}{R^2} \right) \frac{\partial^2}{\partial x^2} + \left(\frac{A'_{22}}{R^2} + \frac{2B'_{22}}{R^3} + \frac{D'_{22}}{R^4} \right) \frac{\partial^2}{\partial \theta^2},$$

$$L_{23} = \left(\frac{A'_{22}}{R^2} + \frac{B'_{22}}{R^3} \right) \frac{\partial}{\partial \theta} - \left(\frac{B'_{22}}{R^3} + \frac{D'_{22}}{R^4} \right) \frac{\partial^3}{\partial \theta^3} - \left(\frac{B'_{12} + 2B'_{66}}{R} + \frac{D'_{12} + 4D'_{66}}{R^2} \right) \frac{\partial^3}{\partial x^2 \partial \theta},$$

$$L_{31} = -\frac{A'_{12}}{R} \frac{\partial}{\partial x} + B'_{11} \frac{\partial^3}{\partial x^3} + \frac{(B'_{12} + 2B'_{66})}{R^2} \frac{\partial^3}{\partial x \partial \theta^2},$$

$$L_{32} = \left(\frac{A'_{22}}{R^2} + \frac{B'_{22}}{R^3} \right) \frac{\partial}{\partial \theta} - \left(\frac{B'_{22}}{R^3} + \frac{D'_{22}}{R^4} \right) \frac{\partial^3}{\partial \theta^3} - \left(\frac{B'_{12} + 2B'_{66}}{R} + \frac{D'_{12} + 4D'_{66}}{R^2} \right) \frac{\partial^3}{\partial x^2 \partial \theta},$$

$$L_{33} = -\frac{A'_{22}}{R^2} + \frac{2B'_{12}}{R} \frac{\partial^2}{\partial x^2} + \frac{2B'_{22}}{R^3} \frac{\partial^2}{\partial \theta^2} - D'_{11} \frac{\partial^4}{\partial x^4} - 2 \frac{D'_{12} + 2D'_{66}}{R^2} \frac{\partial^4}{\partial x^2 \partial \theta^2} - \frac{D'_{22}}{R^4} \frac{\partial^4}{\partial \theta^4},$$

2.3 Solution Methodology

The wave propagation technique has been applied by many scientists to analyse vibrational features of the cylinder shell. Zhang et al. [21], Liu et al. [22], Natsuki et al. [23] and Xuebin [24] are some of them. Same approach is also applied in this manuscript to calculate the natural frequency of the cylindrical shell. Consider the following displacement functions to impart the spatial and temporal variables

$$\left. \begin{aligned} w(x, \theta, t) &= A \cos(n\theta) e^{i(\omega t - k_m x)} \\ v(x, \theta, t) &= B \sin(n\theta) e^{i(\omega t - k_m x)} \\ w(x, \theta, t) &= C \cos(n\theta) e^{i(\omega t - k_m x)} \end{aligned} \right\}, \quad (2.10)$$

in the x , θ and z direction, respectively. Coefficients A, B, C are wave amplitude for different orthogonal coordinates. To denote circumferential wavenumber and axial wave number symbolically, n and k_m is used respectively. The axial wavenumber k_m is different for different kind of boundary conditions. k_m is elected to meet the boundary condition at both the ends of the cylindrical shell and ω denote the natural circular frequency of the shell.

Use Eq. (2.10) into Eq. (2.9) to simplify and rearrange the expressions. Then, to calculate the frequency an equation is formed. This equation would be an eigenvalue problem and can be written as:

$$\begin{bmatrix} C'_{11} & C'_{12} & C'_{13} \\ -C'_{21} & C'_{22} & C'_{23} \\ -C'_{31} & C'_{32} & C'_{33} \end{bmatrix} \begin{bmatrix} A \\ B \\ C \end{bmatrix} = \omega^2 \begin{bmatrix} \rho h & 0 & 0 \\ 0 & \rho h & 0 \\ 0 & 0 & \rho h \end{bmatrix} \begin{bmatrix} A \\ B \\ C \end{bmatrix}, \quad (2.11)$$

where the matrix adjacent to the left hand is stiffness matrix with coefficients C'_{ij} ($i, j = 1, 2, 3$). The square matrix on the right hand side of the frequency equation is the mass matrix which depends upon the shell parameter and boundary conditions which depends on end points of cylindrical shell. The coefficients C'_{ij} are given as:

$$C'_{11} = A'_{11}k_m^2 + \frac{n^2 A'_{66}}{R^2},$$

$$C'_{12} = ink_m \left(\frac{A'_{12} + A'_{66}}{R} + \frac{B'_{12} + 2B'_{66}}{R^2} \right),$$

$$C'_{13} = iK_m \left(\frac{A'_{12}}{R} + B'_{11}k_m^2 + n^2 \frac{B'_{12} + 2B'_{66}}{R^2} \right),$$

$$C'_{22} = n^2 \left(\frac{A'_{22}}{R^2} + \frac{2B'_{22}}{R^3} + \frac{D'_{22}}{R^4} \right) + k_m^2 \left(A'_{66} + \frac{4B'_{66}}{R} + \frac{4D'_{66}}{R^2} \right),$$

$$C'_{23} = n \left(\frac{A'_{22}}{R^2} + \frac{2B'_{22}}{R^3} + n^2 \left(\frac{B'_{22}}{R^3} + \frac{D'_{22}}{R^4} \right) + k_m^2 \left(\frac{B'_{12} + 2B'_{66}}{R} + \frac{D'_{12} + 4D'_{66}}{R^2} \right) \right),$$

$$C'_{33} = \left(\frac{A'_{22}}{R^2} + \frac{2k_m^2}{R} B'_{12} + 2B'_{22} \frac{n^2}{R^3} + D'_{11}k_m^4 + 2n^2k_m^2 \left(\frac{D'_{12} + 4D'_{66}}{R^2} \right) + n^4 \frac{D'_{22}}{R^4} \right).$$

Eq. (2.11) is solved with the help of MATLAB to obtain the frequency related to axial, circumferential and radial displacement.

2.4 Results and Discussions

To verify the accuracy of present results, a comparison is made with the results present in literature for the simply supported-simply supported (S-S) boundary condition. The natural frequency of the cylindrical shell is obtained by using the parameters $E=30 \times 10^6 \text{ lbf in}^{-2}$, $L/R = 4$, $h/R = 1/20$, $\nu=0.3$, $\rho = 7.35 \times 10^{-4} \text{ lbf s}^2 \text{ in}^{-4}$ of the shell. Table 2.1 is a comparison of the present natural frequencies of isotropic cylindrical shell with those obtained by Warburton [20] and Loy [25]. These frequencies are compiled with different axial mode numbers m and simply supported-simply supported (S-S) boundary condition is used. It is found that the natural frequency continuously increases with the increasing number of axial mode number m . Table 2.2 shows the two sets of results of natural frequency of a cylindrical shell with axial mode $m = 1$ and for different circumferential wave number n . It is seen from the Table 2.2, the frequency of the shell first attains its minimum and then arises with the increasing value of n . Moreover, the Table 2.1 and Table 2.2 indicate the small difference in the frequencies with the frequencies obtained by the researchers. The geometrical parameters of the shell are used same as were found in the literature. Then, it may be the effect of two different approaches i.e. wave propagation and the technique used by the researchers. Which proves the accuracy of wave propagation approach.

Variation of natural frequency is also discussed through graphically. In Fig. 2.2 natural frequency is plotted against the circumferential wavenumber n by taking different axial mode and it is noticed that the frequency first attains its lowest value and afterwards it arises with growing worth of circumferential wave number n in all cases of axial mode. Fig. 2.3 illustrates the change in natural frequency against length to radius ratio of simply supported boundary condition. It can be seen from the Fig. 2.3 the natural

Table 2.2 Evaluation of natural frequencies(Hz) versus the number of values of circumferential wavenumber for parameters ($E= 2.1 \times 10^{11}$ N/m², $m= 1$, $L= 0.41$ m, $h = 0.001$ m, $\nu = 0.3$, $\rho = 7850$ kg/m³, $R = 0.3015$ m) of the cylindrical shell.

<i>m</i>	<i>n</i>	Goncalves [26]	Present results	Difference%
1	7	303.35	301.9299	0.47
	8	280.94	278.9986	0.69
	9	288.71	286.3749	0.81
	10	318.40	315.8318	0.81
	11	363.33	360.6421	0.74
	12	419.19	416.4385	0.66
	13	483.51	480.7430	0.57
	14	554.97	552.2161	0.50

2.4 Results and Discussions

To verify the accuracy of present results, a comparison is made with the results present in literature for the simply supported-simply supported (S-S) boundary condition. The natural frequency of the cylindrical shell is obtained by using the parameters $E=30 \times 10^6 \text{ lbf in}^{-2}$, $L/R = 4$, $h/R = 1/20$, $\nu=0.3$, $\rho = 7.35 \times 10^{-4} \text{ lbf s}^2 \text{ in}^{-4}$ of the shell. Table 2.1 is a comparison of the present natural frequencies of isotropic cylindrical shell with those obtained by Warburton [20] and Loy [25]. These frequencies are compiled with different axial mode numbers m and simply supported-simply supported (S-S) boundary condition is used. It is found that the natural frequency continuously increases with the increasing number of axial mode number m . Table 2.2 shows the two sets of results of natural frequency of a cylindrical shell with axial mode $m = 1$ and for different circumferential wave number n . It is seen from the Table 2.2, the frequency of the shell first attains its minimum and then arises with the increasing value of n . Moreover, the Table 2.1 and Table 2.2 indicate the small difference in the frequencies with the frequencies obtained by the researchers. The geometrical parameters of the shell are used same as were found in the literature. Then, it may be the effect of two different approaches i.e. wave propagation and the technique used by the researchers. Which proves the accuracy of wave propagation approach.

Variation of natural frequency is also discussed through graphically. In Fig. 2.2 natural frequency is plotted against the circumferential wavenumber n by taking different axial mode and it is noticed that the frequency first attains its lowest value and afterwards it arises with growing worth of circumferential wave number n in all cases of axial mode. Fig. 2.3 illustrates the change in natural frequency against length to radius ratio of simply supported boundary condition. It can be seen from the Fig. 2.3 the natural

frequency decreases with swelling ratio of length to radius for different values of circumferential wave number. From Figs. 2.2-2.3, it is demonstrated that natural frequency declines with the variation of L/R ratio as circumferential wavenumber.

Table 2.1 Evaluation of natural frequencies(Hz) versus the number of values of axial mode for parameter ($L=8$, $R=2$ in, $\rho = 7.35 \times 10^{-4}$ lbf s² in⁻⁴, $E=30 \times 10^6$ lbf in⁻², $\nu=0.3$) of cylindrical shell.

n	m	Warburton [20]	Loy et al. [25]	Present results
2	1	2046.8	2043.8	2042.7
	2	5637.6	5635.4	5631.9
	3	8935.3	8932.5	8926.4
	4	11405	11407.5	11399.4
	5	13245	13253.2	13243.7
	6	14775	14790.0	14779.9
3	1	2199.3	2195.1	2194.4
	2	4041.9	4035.5	4031.2
	3	6620.0	6614.6	6605.9
	4	9124.0	9121.0	9108.4
	5	11357	11359.0	11343.4
	6	13384	13392.3	13374.9

Table 2.2 Evaluation of natural frequencies(Hz) versus the number of values of circumferential wavenumber for parameters ($E= 2.1 \times 10^{11}$ N/m², $m= 1$, $L= 0.41$ m, $h = 0.001$ m, $\nu = 0.3$, $\rho = 7850$ kg/m³, $R = 0.3015$ m) of the cylindrical shell.

<i>m</i>	<i>n</i>	Goncalves [26]	Present results	Difference%
1	7	303.35	301.9299	0.47
	8	280.94	278.9986	0.69
	9	288.71	286.3749	0.81
	10	318.40	315.8318	0.81
	11	363.33	360.6421	0.74
	12	419.19	416.4385	0.66
	13	483.51	480.7430	0.57
	14	554.97	552.2161	0.50

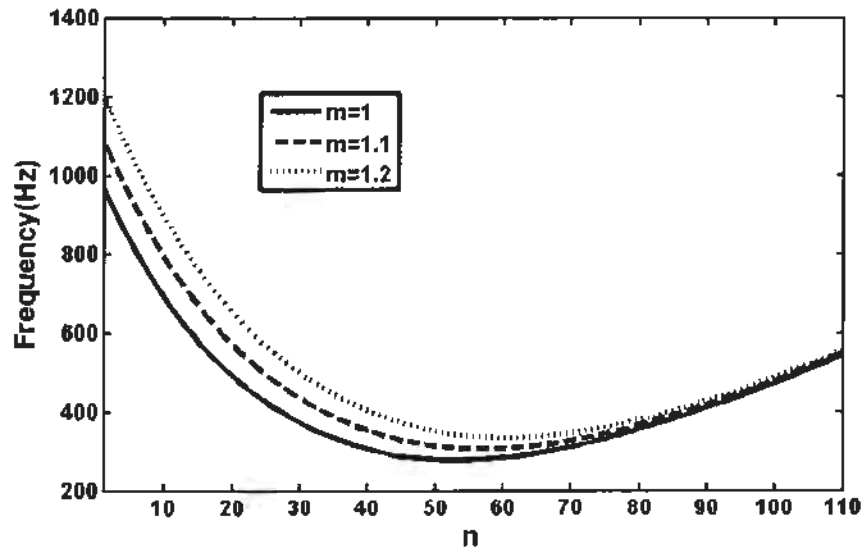


Fig. 2.2. Variation in natural frequency(Hz) ω versus the circumferential wavenumber n when $\rho = 7850$, $m=1$, $L=0.41$, $R = 0.3015$, $E=2.1 \times 10^{11}$, $h=0.001$.

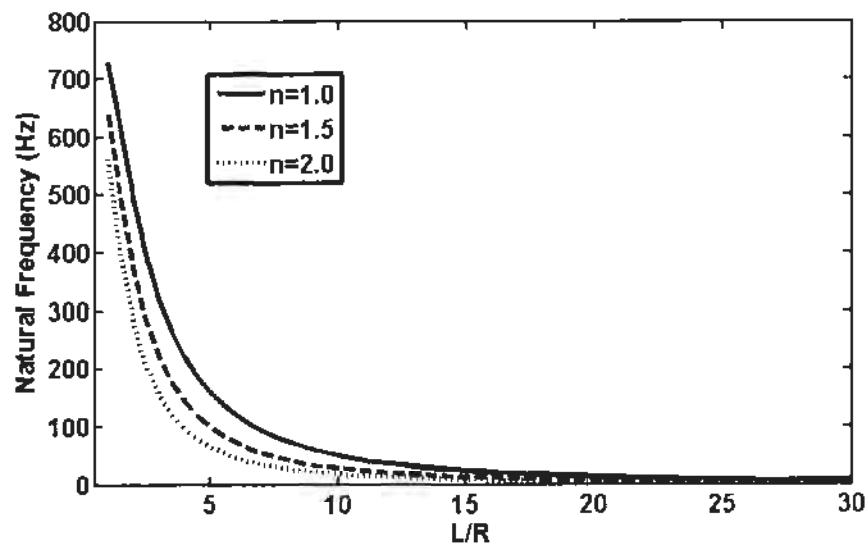


Fig. 2.3. Variation in natural frequency(Hz) ω against the ratio L/R of a cylindrical shell when $L=0.41$, $m=1$, $h=0.001$, $R = 0.3015$, $\rho = 7850$, $E = 2.1 \times 10^{11}$.

2.5 Conclusion

In present study, natural frequency of the cylindrical shell is analysed and simply supported (S-S) boundary condition on both ends of shell is applied. Equations of motion of cylindrical shell are considered using the Love's thin shell theory. To solve the equation of motion, wave propagation approach was applied. Further, MATLAB computation package is used to obtain the numerical results. The obtained results are elaborated through graphically and discussed in detail. Present results are almost similar to the results present in open literature. It is found that natural frequencies of cylindrical shell obtained by using wave propagation approach first decrease up to its minimum value and then increase with ascending values of circumferential wave number n . Another result is also concluded that the length to radius ratio also effects in the frequency of the shell and it descend with increasing value of the radius ratio. This result is checked with different circumferential wavenumber n through tables.

Chapter 3

Vibrational Analysis of Carbon Nanotubes Based on Cylindrical Shell by Inducting Winkler and Pasternak Foundation

3.1 Introduction

This chapter is concerned with the vibrational analysis of CNTs with their all shapes i.e. Armchair, Zigzag and Chiral by employing five different boundary conditions (S-S, C-C, C-F, F-S, C-SI).

3.2 Mathematical Formulation of Equations of Motion

Consider a CNT having geometrical parameters such as length, radius and thickness denoted by L , h and R correspondingly. CNTs have the material properties such as Young's modulus, poisson ratio and mass density denoted by E , ν , ρ respectively. An orthogonal system x , θ and z is established on the middle of the CNTs to show the displacement in the axial, circumferential and radial direction. To relate the displacement in x , θ and z direction consider the function u , v and w .

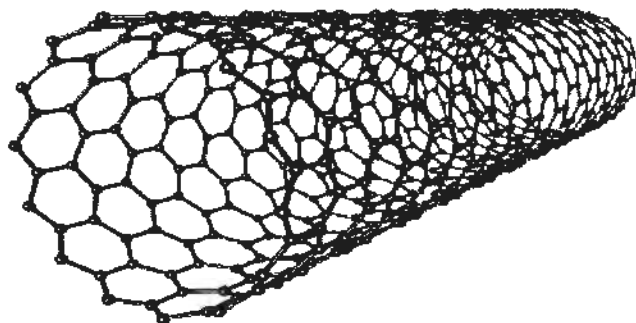


Fig. 3.1. Coordinate system and shell structure of CNT.

Consider the Eqs. (2.1)-(2.3) for the motion CNTs by Love's first shell theory. Equations of motion for both cylindrical shells and carbon nanotubes are taken same because analogousness of the cylindrical shell model and CNTs leads to the wide use of the shell model for CNTs structures. For instance, Yan et al. [27] studied the linear and nonlinear vibration behaviours of double-walled carbon nanotubes based on Donnell's cylindrical shell model. Using the wave propagation approach and substituting moment and force resultants the above equations can be written in the form of differential operators and adding the terms which describe the Winkler and Pasternak foundations ($Kw - G\nabla^2w$) in the z-direction.

$$\left. \begin{aligned} L_{11}u + L_{12}v + L_{13}w &= \rho_t \frac{\partial^2 u}{\partial t^2}, \\ L_{21}u + L_{22}v + L_{23}w &= \rho_t \frac{\partial^2 v}{\partial t^2}, \\ L_{31}u + L_{32}v + L_{33}w &= \rho_t \frac{\partial^2 w}{\partial t^2} + Kw - G\nabla^2w \end{aligned} \right\} \quad (3.4)$$

where G and K are elastic foundations which have been discussed in the chapter 1. The differential operator ∇^2 is defined as:

$$\nabla^2 = \frac{\partial^2}{\partial x^2} + \frac{1}{R} \frac{\partial^2}{\partial \theta^2}, \quad (3.5)$$

along with the differential operator L_{ij} ($i, j = 1, 2, 3$) with respect to x and θ which had been defined in previous chapter.

3.3 Solution Methodology

The equations of motion for a CNT are same as were used for the motion of cylindrical shell. The other parameters like displacement functions, notation for the material properties and displacement functions are also same like the previous equations. So in

order to solve this system the same approach i.e. Wave propagation approach is used.

Displacement function for separating spatial and temporal variables are given as:

$$\left. \begin{aligned} w(x, \theta, t) &= A \cos(n\theta) e^{i(\omega t - k_m x)} \\ v(x, \theta, t) &= B \sin(n\theta) e^{i(\omega t - k_m x)} \\ w(x, \theta, t) &= C \cos(n\theta) e^{i(\omega t - k_m x)} \end{aligned} \right\}, \quad (3.6)$$

in the x , θ and z direction, respectively. Coefficients A , B and C are wave amplitude for different orthogonal coordinates. To denote circumferential wavenumber and axial wave number symbolically, n and k_m are used respectively. The axial wavenumber k_m is different for different kind of boundary conditions. To satisfy the boundary condition at both ends of the cylindrical shell k_m is taken from the following table where ω denotes cylindrical shell's natural circular frequency.

Table 3.1 Boundary conditions for a cylindrical shell

Boundary Conditions	Wavenumbers
Clamped-Free (C-F)	$k_m = (2m - 1)\pi/2L$
Free-Simply Supported (F-S)	$k_m = (4m + 1)\pi/4L$
Simply-Simply Supported (S-S)	$k_m = m\pi/L$
Clamped-Sliding (C-SI)	$k_m = (4m - 1)\pi/4L$
Clamped-Clamped (C-C)	$k_m = (2m + 1)\pi/2L$

One of the k_m is chosen from the above table to fulfil the boundary condition at both ends of the CNT. Further in displacement function ω denote the natural circular frequency of the CNT. Eq. (3.6) is used into Eq. (3.4) to simplify and rearrange. An equation is formed in which frequency is involved. This equation represents an Eigen

value problem and its solution can be obtained by using computer software. The equation is:

$$\begin{bmatrix} C'_{11} & C'_{12} & C'_{13} \\ -C'_{21} & C'_{22} & C'_{23} \\ -C'_{31} & C'_{32} & C'_{33} \end{bmatrix} \begin{bmatrix} A \\ B \\ C \end{bmatrix} = \omega^2 \begin{bmatrix} \rho h & 0 & 0 \\ 0 & \rho h & 0 \\ 0 & 0 & \rho h \end{bmatrix} \begin{bmatrix} A \\ B \\ C \end{bmatrix}, \quad (3.7)$$

where the matrix adjacent to left hand of above equation is stiffness matrix with coefficients $C_{ij}(i, j = 1, 2, 3)$. The square matrix on the right hand of the frequency equation is the mass matrix which depends upon the shell parameters and boundary conditions which depend on ends points of CNT. The coefficients C_{ij} are given as:

$$C'_{11} = A'_{11}k_m^2 + \frac{n^2 A'_{66}}{R^2},$$

$$C'_{12} = ink_m \left(\frac{A'_{12} + A'_{66}}{R} + \frac{B'_{12} + 2B'_{66}}{R^2} \right),$$

$$C'_{13} = iK_m \left(\frac{A'_{12}}{R} + B'_{11}k_m^2 + n^2 \frac{B'_{12} + 2B'_{66}}{R^2} \right),$$

$$C'_{22} = n^2 \left(\frac{A'_{22}}{R^2} + \frac{2B'_{22}}{R^3} + \frac{D'_{22}}{R^4} \right) + k_m^2 \left(A'_{66} + \frac{4B'_{66}}{R} + \frac{4D'_{66}}{R^2} \right),$$

$$C'_{23} = n \left(\frac{A'_{22}}{R^2} + \frac{2B'_{22}}{R^3} + n^2 \left(\frac{B'_{22}}{R^3} + \frac{D'_{22}}{R^4} \right) + k_m^2 \left(\frac{B'_{12} + 2B'_{66}}{R} + \frac{D'_{12} + 4D'_{66}}{R^2} \right) \right),$$

$$C'_{33} = \left(\frac{A'_{22}}{R^2} + \frac{2k_m^2}{R} B'_{12} + 2B'_{22} \frac{n^2}{R^3} + D'_{11}k_m^4 + 2n^2 k_m^2 \left(\frac{D'_{12} + 4D'_{66}}{R^2} \right) + n^4 \frac{D'_{22}}{R^4} + K \right. \\ \left. + G \left(k_m^2 + \frac{n^2}{R^2} \right) \right).$$

Eq. (3.7) is solved by using computer software in order to get the frequency corresponding to axial, circumferential and radial displacement.

3.4 Results and Discussions

In Figs. (3.2)-(3.6) the alteration of natural frequency is drawn against the circumferential wavenumber n for different shapes of CNTs without elastic foundation. The graph describes the behaviour of natural frequency of Armchair, Chiral and Zigzag shapes with five different boundary conditions. Natural frequency of all three shapes of CNTs first decreases and then increases with increasing the value of circumferential wavenumber for different boundary conditions. The properties of CNTs are elaborated in Table 3.2.

In Figs. (3.7)-(3.11) the Change in natural frequency(Hz) is drawn against the circumferential wavenumber n for different shapes of CNT in the presence of elastic foundation. The graph shows the behaviour of natural frequency of Armchair, Chiral and Zigzag shapes with five different boundary conditions. It is detected from the results that natural frequency rises with the variation of circumferential wavenumber for boundary conditions like S-S, C-C, C-F, F-S, C-Sl. In Figs (3.12)-(3.14) natural frequencies (Hz) of CNT against length-to- radius ratio for various values of axial wavenumber m are sketched. The graph describes the behaviour of natural frequency of Armchair, Chiral and Zigzag shapes. Natural frequency decreases with increasing L/R ratio in all shapes of CNTs. The elastic foundation is also taken into account. The results demonstrate that natural frequencies of armchair, zigzag and chiral decreases with the variation of L/R , whereas opposite trend is seen for axial wavenumber m . It is also noted that CNTs with chiral shape obtained maximum frequency followed by zigzag and armchair.

Table 3.2. Material properties of CNT [26].

Tube (n, m)	Armchair (10,10)	Zigzag (10, 0)	Chiral (10, 2)
Radius(R)	0.6427nm	0.3713nm	0.4134nm
Wall Thickness(h)	0.1232nm	0.0878nm	0.0974nm
Density(ρ)	1.33g/cm ³	2.3g/cm ³	1.40g/cm ³
Poison Ratio(ν)	0.180	0.265	0.209
Young's modulus(E)	2.618TPa	3.939TPa	3.465TPa
Length(L)	6.427nm	3.713nm	4.134nm

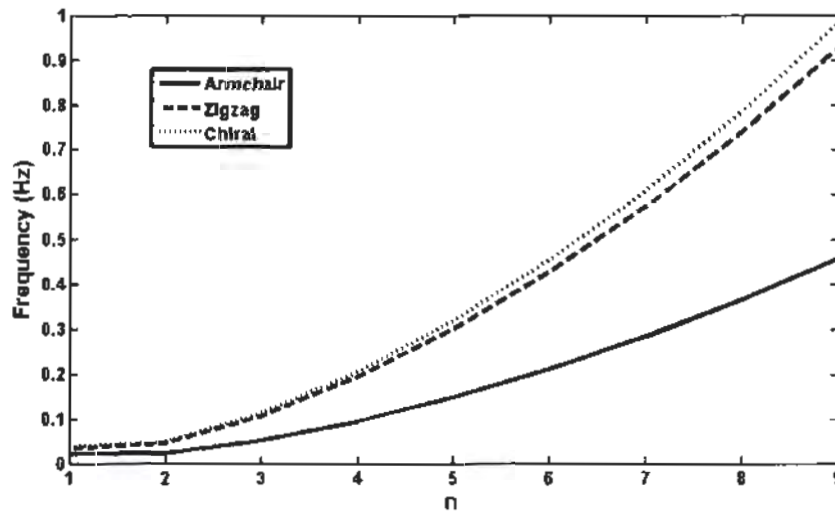


Fig. 3.2. Variation in natural frequency(Hz) against circumferential wavenumber n , for S-S boundary condition, when $m = 1, G = 0, K = 0$.

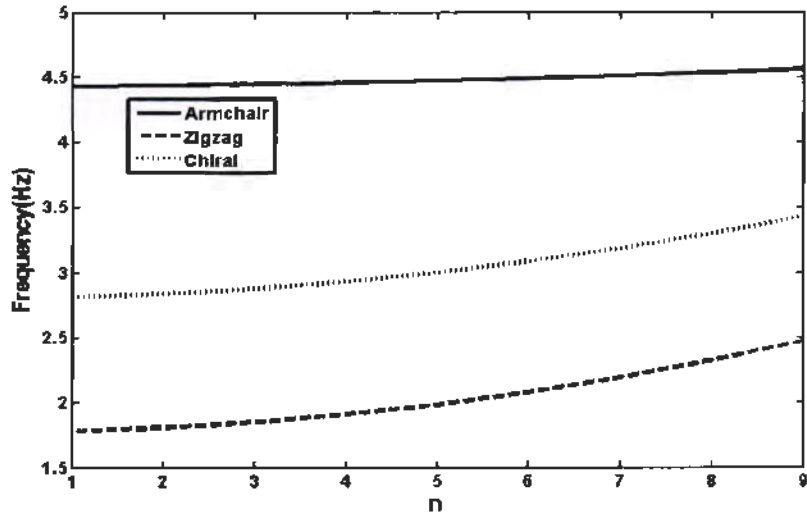


Fig. 3.3. Variation in natural frequency(Hz) against circumferential wavenumber n , for C-C boundary condition, when $m = 1, G = 0, K = 0$.

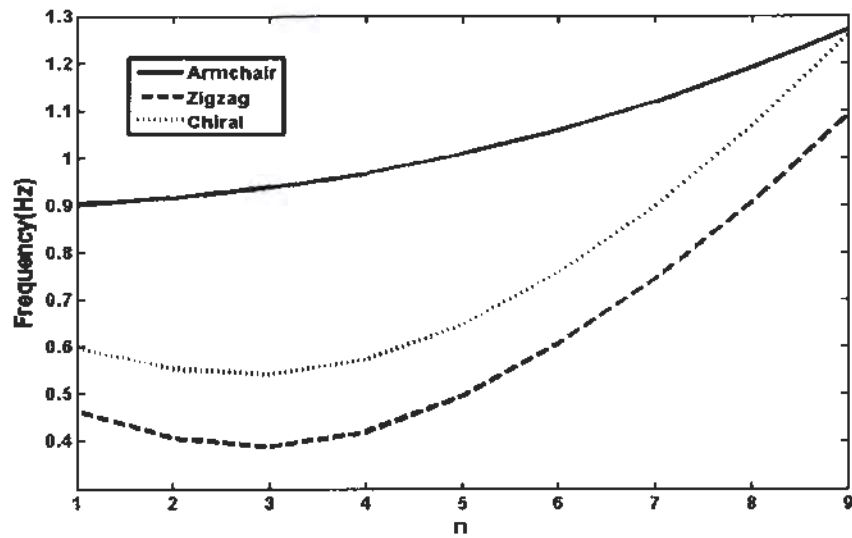


Fig. 3.4. Variation in natural frequency(Hz) against circumferential wavenumber n , for C-F boundary condition, when $m = 1, G = 0, K = 0$.

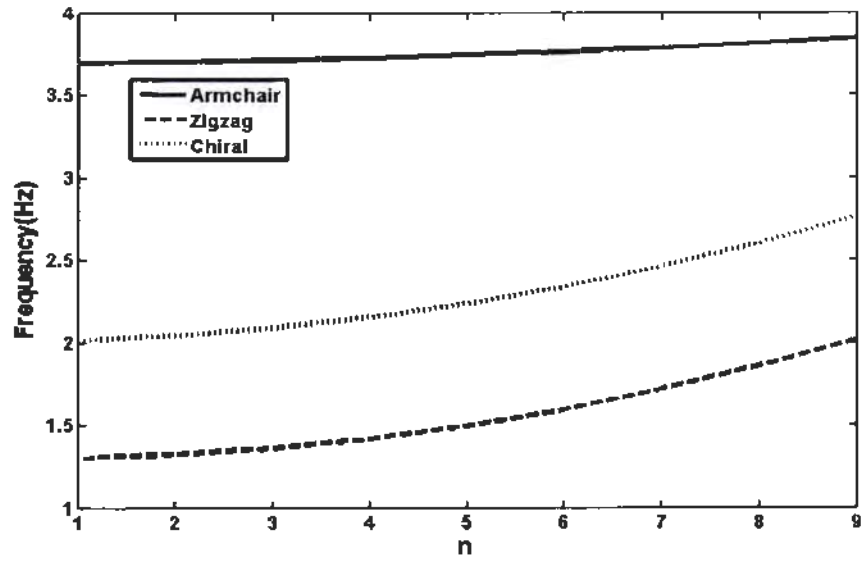


Fig. 3.5. Variation in natural frequency(Hz) against circumferential wavenumber n , for C-SI boundary condition, when $m = 1, G = 0, K = 0$.

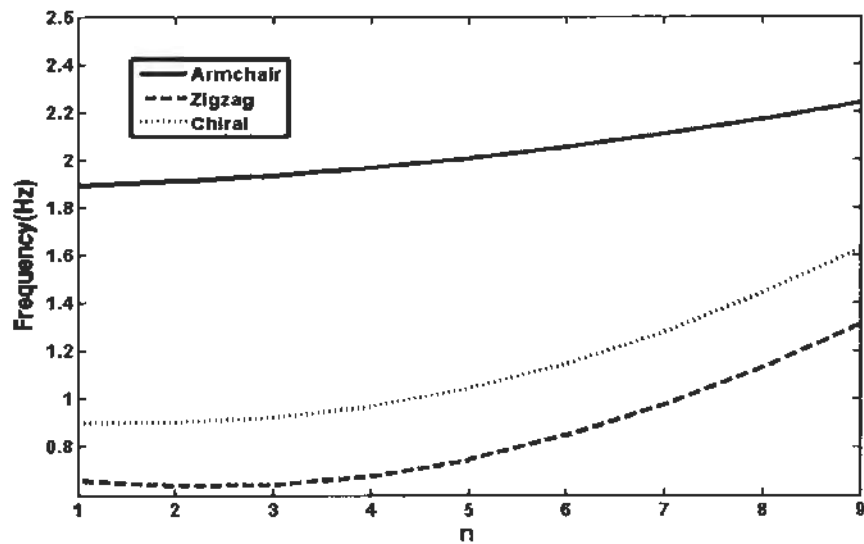


Fig. 3.6 Variation in natural frequency(Hz) against circumferential wavenumber n , for F-S boundary condition, when $m = 1, G = 0, K = 0$.

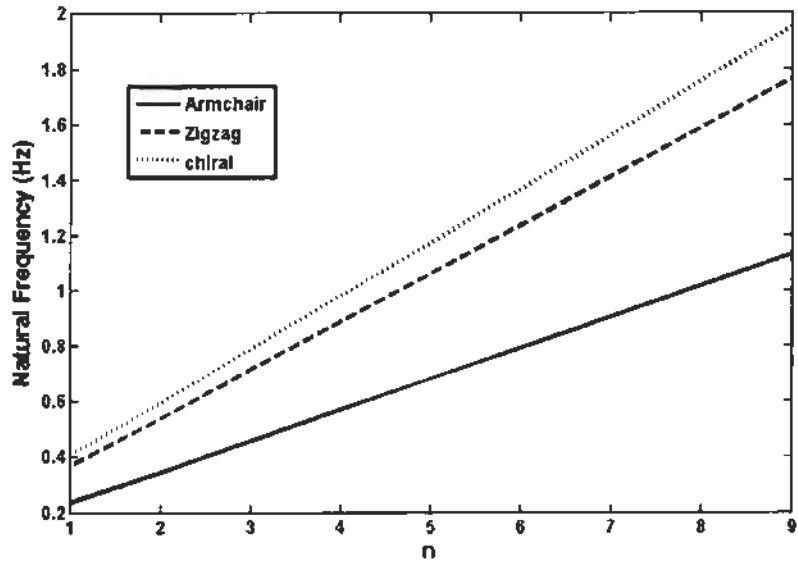


Fig. 3.7 Variation in natural frequency(Hz) against circumferential wavenumber n , for S-S boundary condition, when $m = 1, G = 1.5 \times 10^7, K = 5.5 \times 10^7$.

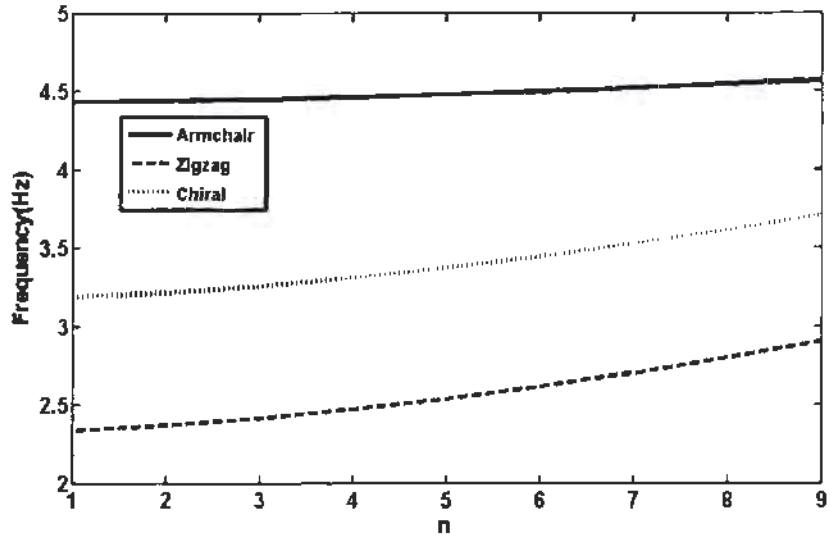


Fig 3.8 Variation in natural frequency(Hz) against circumferential wavenumber n , for C-C boundary condition, when $m = 1, G = 1.5 \times 10^7, K = 5.5 \times 10^7$.

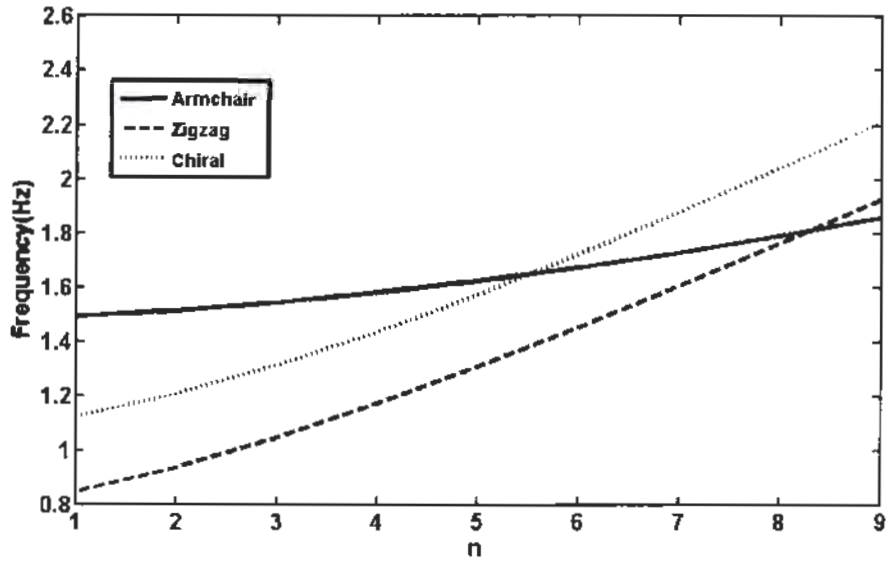


Fig. 3.9 Variation in natural frequency(Hz) against circumferential wavenumber n , for C-F boundary condition, when $m = 1, G = 1.5 \times 10^7, K = 5.5 \times 10^7$

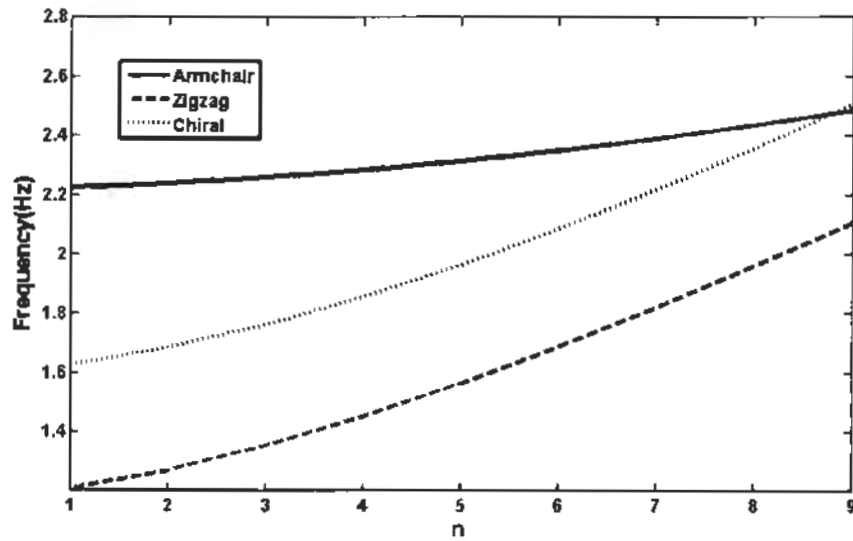


Fig. 3.10 Variation in natural frequency(Hz) against circumferential wavenumber n , for F-S boundary condition, when $m = 1, G = 1.5 \times 10^7, K = 5.5 \times 10^7$.

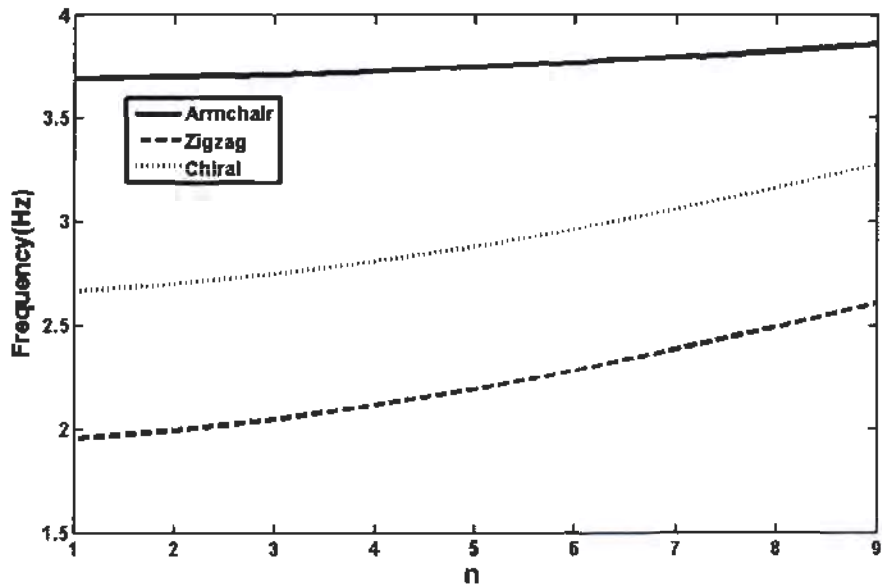


Fig. 3.11 Variation in natural frequency(Hz) against circumferential wavenumber n , for C-SI boundary condition, when $m = 1, G = 1.5 \times 10^7, K = 5.5 \times 10^7$.

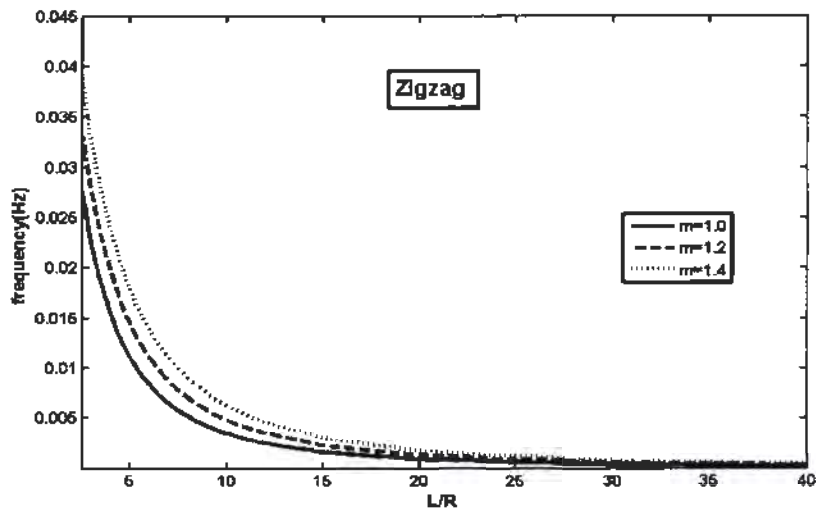


Fig. 3.12 Variation in natural frequency(Hz) of Zigzag shape CNT against length to radius ratio L/R when $n = 1, m = 1, G = 1.5 \times 10^7, K = 5.5 \times 10^7$.

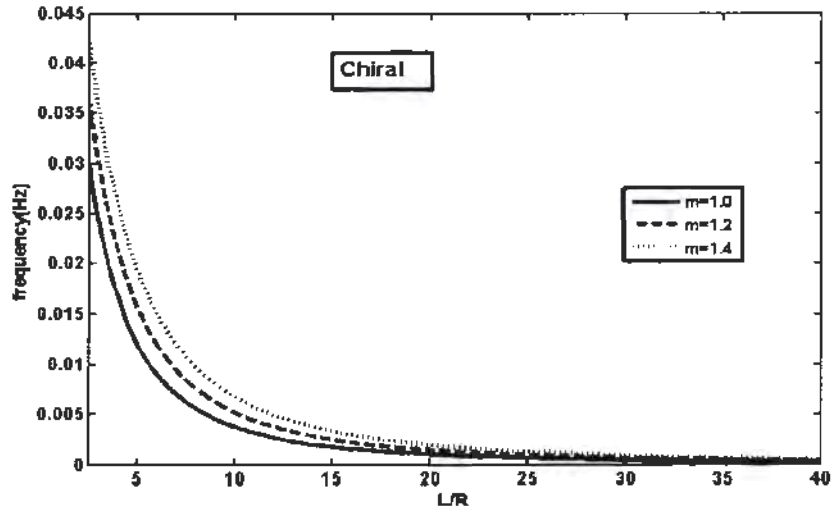


Fig. 3.13 Variation in natural frequency(Hz) of Chiral shape CNT against length to radius ratio L/R when $n = 1, m = 1, G = 1.5 \times 10^7, K = 5.5 \times 10^7$.

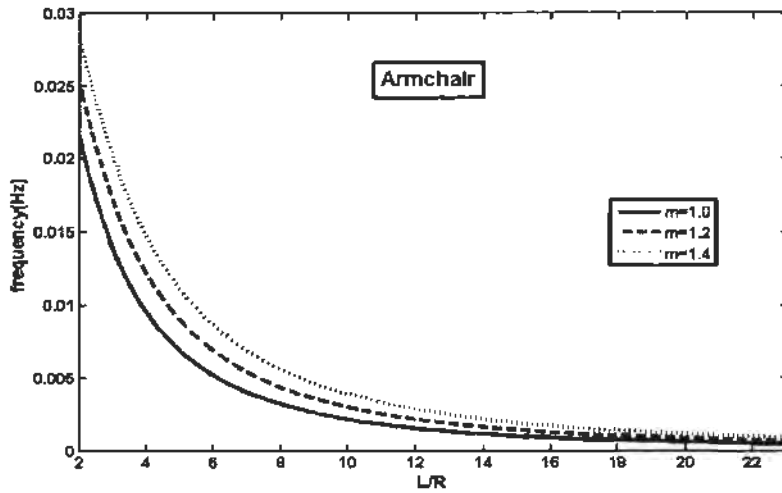


Fig. 3.14 Variation in natural frequency(Hz) of Armchair shape CNT against length to radius ratio L/R when $n = 1, m = 1, G = 1.5 \times 10^7, K = 5.5 \times 10^7$.

3.5 Conclusion

The purpose of the study is to determine the natural frequencies of CNTs based on cylindrical shell by employing wave propagation approach for different boundary conditions. The shapes of CNTs like Armchair, Zigzag and chiral are also elaborated for five different boundary conditions S-S, C-C, C-F, F-SI and C-S, respectively. Natural frequencies are analysed with and without elastic foundation. Obtained results are sketched graphically for each boundary condition.

References

- [1] S. Iijima, Helical microtubules of graphitic carbon, *Nature* 345, 56–58 (1991).
- [2] M. R. Falvo, G. J. Clary, R. M. Taylor II, V. Chi, F. P. Brooks, S. Washburn, Bending and buckling of carbon nanotubes under large strain, (1997).
- [3] C. Y. Li and T. A. Chou, A structural mechanics approach for the analysis of carbon nanotubes, *International Journal of Solids and Structures* 40, 2487–2499 (2003).
- [4] A. Sakhaee-Pour, M. T. Ahmadian, and A. Vafai, Vibrational analysis of single-walled carbon nanotubes using beam element, *Thin-Walled Structures* 47, 646–652 (2009).
- [5] B. I. Yakobson, C. J. Brabee, and J. Bernhole, Vibrational analysis of single-walled carbon nanotubes using beam element, *Phys. Rev. Lett.* 76, 2511–2514 (1996).
- [6] J. C. Hsu, R. P. Chang, and W. J. Chang, Resonance frequency of chiral single-walled carbon nanotubes using Timoshenko beam theory, *Physics Letters A* 372, 2757–2759 (2008).
- [7] T. Vodenitcharova and L. C. Zhang, Resonance frequency of chiral carbon nanotubes using Timoshenko beam theory, *Phys. Rev. B* 68, 165401 (2003).
- [8] G. X. Cao, X. Chen, and J. W. Kysar, Effective wall thickness of single walled carbon nanotubes, *Phys. Rev. B* 72, 195412 (2005).
- [9] R. M. Moghadam, S. A. Hosseini, and M. Salehi, The influence of stone thrower wales defect on vibrational characteristics of single walled carbon nanotubes, *Physica E* 62, 80–89 (2014).
- [10] Gao B., Enhanced Saturation Lithium Composition in Ball Milled Single Walled Carbon Nanotubes. *Chemical Physics Letters* 327, 69. (2000).
- [11] P. Poncharal, Z. L. Wang, D. Ugarte, and W. A. De Heer, Numerical analysis of the vibrational frequency of deformed single-wall carbon nanotubes, *Science* 283, 1513–1516 (1999).

- [12] M. M. J. Treacy, T. W. Ebbesen, and J. M. Gibson, Electrostatic deflections and electro mechanics resonances of carbon nanotubes, *Nature* 381, 678–680 (1996).
- [13] Q. Zhao, Z. H. Gan, and O. K. Zhuang, Exceptionally high Young's modulus observed for individual carbon nanotubes, *Electro analysis* 14, 1609–1613 (2002).
- [14] C. Y. Li and T. W. Chou, Vibrational behaviour of carbon nanotubes based nano mechanical resonator, *Appl. Phys. Lett.* 84, 121–123 (2003).
- [15] Li Chunyu and T.-W. Chou, Vibrational behaviour of single walled carbon nanotubes based on cylindrical shell model using wave propagation model, *Nano-Mechanics of Materials and Structures*, Springer pp. 55–65 (2006).
- [16] C. Y. Li and T. W. Chou, Single walled carbon nanotubes as ultrahigh frequency nano mechanical resonator, *Phys. Rev. B* 68, 073405 (2003).
- [17] R. F. Gibson, E. O. Ayorinde, and Y. F. Wen, Vibration of carbon nanotubes and their composites, *Composite Science and Technology* 67, 1–28 (2007).
- [18] A. Swain, T. Roy, and B. K. Nanda, Vibrational behaviour of single walled carbon nanotubes based on cylindrical shell using wave propagation method, *International Journal on Theoretical and Applied Research in Mechanical Engineering* 2(4), 129–133 (2013).
- [19] A. Fereidoon, R. Rafiee, and R. M. Moghadam, A modal analysis of carbon nanotubes reinforced polymer by using a multi scale finite element method, *Mechanics of Composite Materials* 49(3) (2013).
- [20] Warburton, G.B. Vibration of thin cylindrical shells. *J. Mech. Eng. Sci.* 7, 399–407 (1965).
- [21] Zhang, X.M., Liu, G.R., Lam, K.Y., Vibration analysis of cylindrical shells using the wave propagation approach. *J. Sound Vib.* 239(3), 397–401 (2001).

- [22] Liu, J.X., Li, T.Y., Liu, T.G., Yan, J., Vibration characteristic analysis of buried pipes using the wave propagation approach. *Appl. Acoust.* 66, 353–364 (2005).
- [23] Natsuki, T., Ni, Q.Q., Endo, M., Vibrational analysis of fluid-filled carbon nanotubes using the wave propagation approach. *Appl. Phys.* 90, 441–445 (2008).
- [24] Xuebin, L., Study on free vibration analysis of circular cylindrical shells using wave propagation. *J. Sound Vib.* 311, 667–682 (2008).
- [25] Loy, C.T., Lam, K.Y., Vibration of cylindrical shells with ring support. *Int. J. Mech. Sci.* 39(4), 371–455 (1997).
- [26] Goncalves, P.B., da Silva, F.M.A., del Prado, Z.J.G.N.: Transient stability of empty and fluid-filled cylindrical shells. *J. Braz. Soc. Mech. Sci. Eng.* xxviii (3), 331–338 (2006).
- [27] Y. Yan, L.X. Zhang, W.Q. Wang, Dynamical mode transitions of simply supported double-walled carbon nanotubes based on an elastic shell model, *J. Appl. Phys.* 103 113523 (2008).